Inherent Sex Differences in the Expression of the Endocannabinoid System within V1M Cortex and PAG of Sprague Dawley Rats

Aidan Levine (aidanlevine@email.arizona.edu)
University of Arizona Arizona Health Sciences Center: The University of Arizona Health Sciences
https://orcid.org/0000-0003-1808-5228
Erika Liktor-Busa
University of Arizona Arizona Health Sciences Center: The University of Arizona Health Sciences
Austin A Lipinski
University of Arizona Arizona Health Sciences Center: The University of Arizona Health Sciences
Sarah Couture
University of Arizona Arizona Health Sciences Center: The University of Arizona Health Sciences
Shreya Balasubramanian
University of Arizona Health Sciences Center: The University of Arizona Health Sciences
Sue A Aicher
OHSU: Oregon Health & Science University
Paul R Langlais
University of Arizona Arizona Health Sciences Center: The University of Arizona Health Sciences
Todd W Vanderah
University of Arizona Arizona Health Sciences Center: The University of Arizona Health Sciences
Tally M Largent-Milnes
University of Arizona Arizona Health Sciences Center: The University of Arizona Health Sciences

Research Article

Keywords: sex differences, endocannabinoids, 2-arachidonoylglycerol, anandamide, migraine, pain, proteomics, periaqueductal grey

Posted Date: June 11th, 2021

DOI: https://doi.org/10.21203/rs.3.rs-606890/v1

Abstract

Background: Several chronic pain disorders, such as migraine and fibromyalgia, have an increased prevalence in the female population. The underlying mechanisms of this sex-biased prevalence have yet to be thoroughly documented but could be related to endogenous differences in neuromodulators in pain networks, including the endocannabinoid system. The cellular endocannabinoid system is comprised of the endogenous lipid signals 2-AG (2-arachidonoylglycerol) and AEA (anandamide); the enzymes that synthesize and degrade them; and the cannabinoid receptors. The relative prevalence of different components of the endocannabinoid system in specific brain regions may alter responses to endogenous and exogenous ligands.

Methods: Brain tissue from naïve male and female Sprague Dawley rats was harvested from V1M cortex, periaqueductal gray, trigeminal nerve, and trigeminal nucleus caudalis. Tissue was analyzed for relative levels of endocannabinoid enzymes, ligands, and receptors via mass spectrometry, unbiased proteomic analysis, and immunohistochemistry.

Results: Mass spectrometry revealed cortical AEA levels were significantly higher in males compared to females ($p<0.001$), whereas 2-AG levels in periaqueductal grey were significantly higher in females compared to males ($p<0.0001$). Immunohistochemistry followed by unbiased proteomics confirmed the prevalence of 2-AG-endocannabinoid system enzymes in the female PAG.

Conclusions: Our results suggest that sex differences exist in the endocannabinoid system in two CNS regions relevant to cortical spreading depression (V1M cortex) and descending modulatory networks in pain/anxiety (PAG). These basal differences in endogenous endocannabinoid mechanisms may facilitate the development of chronic pain conditions and may also underlie sex differences in response to therapeutic intervention.

Background

Chronic pain disorders affect roughly 20% of adults in the United States, with an increased prevalence in the female population [1]. While the pathogenesis and treatment for certain chronic pain states (i.e., rheumatoid arthritis), have been well documented [2], those of functional chronic pain disorders, such as migraine and fibromyalgia remain elusive. One proposed hypothesis for the pathogenesis of functional pain disorders is the theory of Clinical Endocannabinoid Deficiency (CED) [3].

CED describes chronically low levels of the two main endogenous cannabinoids (eCBs), 2-arachidonoylglycerol (2-AG) and anandamide (AEA), in platelets and the CSF of migraine patients. The endocannabinoid system (ECS) includes the enzymes responsible for the synthesis and degradation of 2-AG and AEA which are primarily synthesized from cellular lipid membranes via the enzymes diacylglycerol lipase (DAGL) and N-acyl-phosphatidylethanolamine hydrolyzing phospholipase D (NAPE-PLD), respectively [4, 5]. The degradation of 2-AG is primarily accomplished via monoacylglycerol lipase (MAGL) and α/β-hydrolase-6 (ABHD6), and that of AEA is performed primarily by fatty acid amide

hydrolase (FAAH) [4]. Expression of the ECS components is brain region and cell-type selective. For example, expression of MAGL is reported to be mainly presynaptic at extrasynaptic regions rich in CB_1R [6] whereas DAGL and ABHD6 are primarily post-synaptic [7, 8]. DAGL, MAGL, and ABHD6 enzymes are reportedly expressed by glial cells [9]. Both 2AG and AEA act on the cannabinoid receptors CB1 and CB2. CB1 represents the primary cannabinoid receptor in the central nervous system (CNS) [4], while CB2 receptors are reported in glial cells and in some neurons [10]. Activation of these receptors reduces neurotransmitter release at glutamatergic and GABA-ergic synapses and inhibits inflammatory responses [11–15].

While the mechanisms driving functional pain disorders remain debated, there is general agreement within the literature of the importance of pain-relevant regions in the central nervous system [16–18]. Regions of interest in pain sensation and modulation include several cortical areas as well as the periaqueductal grey (PAG). Canonically, pain signals are interpreted and modulated by cortical regions [19, 20], which then project to the PAG. Neurons in the PAG project to the rostral ventral medulla (RVM), which in turn projects to the dorsal horn to modulate afferent pain sensations from the spinal cord and trigeminal nucleus caudalis [21–23]. During migraine with aura, the cortical spreading depression events originating in the V1M cortex are thought to underlie visual aura; these CSD events also lead to indirect activation of the PAG [18]. Thus, the PAG and V1M cortex represent relevant areas of interest for examination of role of the ECS in pain signaling.

As functional pain states, including migraine, show an increased prevalence in the female population [1, 24, 25], physiologic differences in expression and localization of ECS components between male and females may underscore the female prevalence of these disorders. Thus, these studies tested whether ECS expression differed between male and female rats in a regionally selective manner in the descending pain pathways that are implicated in chronic pain disorders. Utilizing mass spectrometry, the levels of 2-AG and AEA were quantified in the V1M Cortex and PAG, as a nucleus implicated in the descending pain modulatory pathways. DAGL, MAGL, ABHD6, NAPE-PLD, FAAH, CB1, and CB2 expression and localization were determined using immunohistochemistry of the PAG using the occipital cortex (V1M), a site often associated with the induction of cortical spreading depression events linked to migraine aura, for comparison. Levels of enzyme and receptor expression, as well as localization, varied by central nervous system region and sex. These data suggest differences between the male and female brain composition of the ECS in brain regions associated with pain modulation that may underlie the sex differences in some pain etiologies, as well as pharmacological responsivity.

Materials And Methods

Animals

Female and male Sprague Dawley rats (7-8 weeks old) were purchased from Envigo (Indianapolis, IN) and housed in a climate-controlled room on a regular 12/12 h light/dark cycle with lights on at 7:00 am with food and water available *ad libitum*. Animals were housed three to a cage. All procedures were

performed during the 12-hour light cycle and according to the policies and recommendations of the International Association for the Study of Pain, the NIH guidelines for laboratory animals, with IACUC approval from the University of Arizona. Animal numbers required to achieve statistical power for each assay were determined by G.Power3.1 in alignment with NIH policy (NOT-OD-15-102) such that differences of 20% were detected with 80% power at a significance level of 0.05 [26].

Harvest of tissue samples

Each rat was anesthetized with ketamine:xylazine mix (80:10 mg/kg, i.p.) then transcardially perfused with ice cold 0.1 M phosphate buffer at a rate of 3.1 mL/min for 10 min. After decapitation, spatially discrete brain regions involved in pain signaling (occipital V1M cortex (Ct), ventrolateral periaqueductal gray (vlPAG), trigeminal nucleus caudalis (Vc), and trigeminal ganglia (TG)) were harvested, flash frozen in liquid nitrogen, and stored at -80°C until preparation.

Immunohistochemistry and microscopy

Naïve rats were anesthetized with ketamine:xylazine mix (80:10 mg/kg, i.p.) and then received transcardial perfusion with 0.1M phosphate buffered saline (PBS) followed by 4% paraformaldehyde (PFA) diluted in 0.1M phosphate buffer. Brains were removed and post-fixed 2 hours in 4% PFA, then transferred to 30% sucrose in PBS overnight. Brains were then flash frozen and cut in 40-micron coronal slices using a microtome (Microm HM 525). Free-floating sections were then washed in 0.1M Tris Saline solution (TS) before and after every incubation. First, sections were incubated for 1 hour with 0.5% bovine serum albumin (BSA) in 0.1M TS as a blocking solution, then adjacent sections through each brain region of interest were incubated for 48 hours in primary antibody dilutions as follows: chicken anti-glial fibrillary acidic protein (1:500, Invitrogen PA1-10004), mouse anti-Iba1 (1:300, Invitrogen MA5-27726), goat anti-MAGL (1:250, Abcam 77398), goat anti-DAGL (1:500, Abcam 81984), rabbit anti-CB1R (1:250, Abcam 23703), rabbit anti-FAAH (1:135, Invitrogen PA5-52433), rabbit anti-NAPE-PLD (1:500, Invitrogen PA5-72923), or rabbit anti-ABHD6 (1:250, Invitrogen PA5-38999). Primary antibody dilutions were performed in 0.1% BSA/.25% Triton in 0.1M TS. Tissue sections were rinsed thoroughly in TS then incubated in the dark for 2 hours with the appropriate fluorescently conjugated secondary antibodies as follows (all secondary dilutions were 1:400): AlexaFluor™ 488 Goat anti-chicken (Invitrogen A-11039), AlexaFluor™ 647 Goat anti-chicken (Invitrogen A-21449), AlexaFluor™ 568 Donkey anti-mouse (Invitrogen A-10037), AlexaFluor™ 488 Donkey anti-rabbit (Invitrogen A-21206), or AlexaFluor™ 647 Donkey anti-goat (Invitrogen A-32849). Secondary antibody dilutions were performed in 0.1% BSA in 0.1M TS. Tissue sections were then washed with 0.1M TS followed by 0.1M PB. Finally, tissue sections were incubated for 30 minutes in NeuroTrace™ 435/455 Blue Fluorescent Nissl Stain (1:200, Invitrogen N-21479) in 1X PBS. Slices were then mounted and coverslipped with ProLong™ Gold antifade reagent w/o DAPI. Epifluorescence images were obtained on an ECHO Revolve microscope and high-resolution images were obtained on a Zeiss Elyra S.1 structured illumination microscope. Image analysis was performed with

either ZEN 3.1 Blue software (Carl Zeiss. Jena, Germany) or FIJI ImageJ (https://imagej.net/Fiji) [27]. Within Zen Blue, z-stacks were first processed with a structured illumination Fourier transform followed by a channel alignment algorithm. Z-stacks were then resolved into high-resolution 2D images via extended depth of focus (EDF) and Denoising processing. The colocalization function within the software was then utilized to quantify fluorescent pixels, and thresholds were set to include appropriate pixel intensities. Colocalization and pixel area data were then extracted from these images. Within ImageJ, semi-quanititative analysis of protein expression was performed as previously described [28]. As the proteins of interest exist within extracellular and perisynaptic spaces, whole slide images were analyzed. In order to accommodate for differences in staining, fluorescence intensity, and neuronal soma captured between users, a nissl stain for soma was used as a standard to correct image intensity as previously described [29]. Fixed regions of tissue were imaged and quantified by an observer blind to experimental condition; threshold was similar for all samples and results are expressed as relative immunoreactivity corrected to mean Nissl immunoreactivity. All image analyses were performed in triplicate.

Quantification of 2-AG and AEA by LC-MS

The brain samples for LC-MS were purified by organic solvent extraction, as described by Wilkerson et al. [30]. Briefly, tissues were harvested, snap-frozen in pre-weighted tubes, and stored at -80°C. On the day of processing, tissues were weighed and homogenized in 1 ml of chloroform/methanol (2:1 v/v) supplemented with phenylmethylsulfonyl fluoride (PMSF) at 1mM final concentration to inhibit the degradation by endogenous enzymes. Dounce homogenizer was used for homogenization. Homogenates were then mixed with 0.3 ml of 0.7% w/v NaCl, vortexed, and then centrifuged for 10 min at 3200 × g at 4°C. The aqueous phase plus debris was collected and extracted two more times with 0.8 ml of chloroform. The organic phases from the three extractions were pooled and internal standard was added to each sample. Mixed internal standard solutions were prepared by serial dilution of AEA-d4 and 2-AG-d5 in acetonitrile. The organic solvents were evaporated under nitrogen gas and 6 uL of 30% glycerol in methanol per sample was added before evaporation. Dried samples were reconstituted with 0.2 ml of chloroform and mixed with 1 ml of ice-cold acetone to precipitate proteins. The mixtures were then centrifuged for 5 min at 1800 × g at 4°C. The organic layer of each sample was collected and evaporated under nitrogen.

Analysis of 2-AG and AEA was performed on an Ultivo triple quadrupole mass spectrometer combined with a 1290 Infinity II UPLC system (Agilent, Palo Alto, CA). The instrument was operated in electrospray positive mode with a gas temperature of 150°C at a flow of 5L/min, nebulizer at 15 psi, capillary voltage of 4500V, sheath gas at 400°C with a flow of 12L/min and nozzle voltage of 300V. Transitions monitored were 348.3→287.3 and 62, 352.3→287.4 and 65.9, 379.3→287.2 and 269.2, and 384.3→287.2 and 296.1 for AEA, AEA-d4, 2-AG, and 2-AG-d5. The first fragment listed was used for quantification and the second fragment was used for confirmation. The first 3 minutes of analysis time was diverted to waste. Chromatographic separation was achieved using an isocratic system of 21% 1mM ammonium fluoride and 79% methanol on an Acquity UPLC BEH C-18 1.7um, 2.1x100 mm column (Waters, Milford, MA)

maintained at 60°C. After each injection, the column was washed with 90% methanol for one minute then re-equilibrated for 5 minutes prior to the next injection. Samples were maintained at 4°C. Mixed calibration solutions were prepared by serial dilution of AEA and 2-AG stock solutions in 80% acetonitrile. Calibration curves were prepared for each analysis by adding 10 µl internal standard solution to 20 µl standard solution. Prior to sample analysis, 200 µl of 80:20 acetonitrile:water was added to dried samples which were then vortexed and sonicated. The samples were centrifuged at 15800 x g at 4°C for 5 min. Supernatant was transferred to autosampler vials and 5 µl was injected for analysis.

Proteome analysis of naive PAG

To determine sex differences in the PAG proteome of rats, tissue samples were harvested as described above. The samples were lysed in RIPA-style lysis buffer, containing phosphatase and protease inhibitors (BiMake). The samples were sonicated three times, with one second pulses, followed by centrifugation at 15,000 x g for 10 minutes at 4 °C. The supernatant was collected, BCA assay (Pierce™ BCA Protein Assay Kit, Thermo Scientific) was performed to determine the protein content, then 200µg of the lysate supernatant was separated on a 10% SDS-PAGE gel and stained with Bio-Safe Coomassie G-218250 Stain. Each lane of the SDS-PAGE gel was cut into six slices. The gel slices were subjected to trypsin digestion and the resulting peptides were purified by C18-based desalting exactly as previously described [31,32].

HPLC-ESI-MS/MS was performed in positive ion mode on a Thermo Scientific Orbitrap Fusion Lumos tribrid mass spectrometer fitted with an EASY-Spray Source (Thermo Scientific, San Jose, CA). NanoLC was performed exactly as previously described [31,32].Tandem mass spectra were extracted from Xcalibur 'RAW' files and charge states were assigned using the ProteoWizard 3.0 msConvert script using the default parameters. The fragment mass spectra were searched against the *Mus musculus* and *Rattus norvegicus* SwissProt_2018_01 databases using Mascot (Matrix Science, London, UK; version 2.6.0) using the default probability cut-off score. The search variables that were used were: 10 ppm mass tolerance for precursor ion masses and 0.5 Da for product ion masses; digestion with trypsin; a maximum of two missed tryptic cleavages; variable modifications of oxidation of methionine and phosphorylation of serine, threonine, and tyrosine. Cross-correlation of Mascot search results with X! Tandem was done with Scaffold (version Scaffold_4.8.7; Proteome Software, Portland, OR, USA). Probability assessment of peptide assignments and protein identifications were made using Scaffold. Only peptides with ≥ 95% probability were considered.

Progenesis QI for proteomics software (version 2.4, Nonlinear Dynamics Ltd., Newcastle upon Tyne, UK) was used to perform ion-intensity based label-free quantification. In brief, in an automated format, .raw files were imported and converted into two-dimensional maps (y-axis = time, x-axis =m/z) followed by selection of a reference run for alignment purposes. An aggregate data set containing all peak information from all samples was created from the aligned runs, which was then further narrowed down by selecting only +2, +3, and +4 charged ions for further analysis. The samples were then grouped and a

peak list of fragment ion spectra from only the top eight most intense precursors of a feature was exported in Mascot generic file (.mgf) format and searched against the *Mus musculus* and *Rattus norvegicus* SwissProt_2018_01 database using Mascot (Matrix Science, London, UK; version 2.4). The search variables that were used were: 10 ppm mass tolerance for precursor ion masses and 0.5 Da for product ion masses; digestion with trypsin; a maximum of two missed tryptic cleavages; variable modifications of oxidation of methionine and phosphorylation of serine, threonine, and tyrosine; 13C=1. The resulting Mascot .xml file was then imported into Progenesis, allowing for peptide/protein assignment, while peptides with a Mascot Ion Score of <25 were not considered for further analysis. Protein quantification was performed using only non-conflicting peptides and precursor ion-abundance values were normalized in a run to those in a reference run (not necessarily the same as the alignment reference run). Principal component analysis and unbiased hierarchal clustering analysis (heat map) was performed in Perseus [33,34] while Volcano plots were generated in RStudio.

Data Analysis and Statistics

GraphPad Prism 7.0 software (GraphPad Software) was used for statistical analysis. Unless otherwise stated, the data were expressed as mean ± SEM. Molecular studies were compared by RM two-way ANOVA, where the within variable was neural region and between variable was sex; the interaction between the two variables was assessed as well via post-hoc analysis. Mixed- model analyses were done when appropriate. Differences were considered significant if $p \leq 0.05$ to give 80% power (GPower 3.1). Statistics were performed according to recommendations of the UA Stats Consulting laboratory.

Results

LC-MS analysis of endocannabinoids (eCBs) in female and male tissue

We examined the total level of the primary eCBs, AEA and 2-AG, in V1M cortex, PAG, Vc, and TG of male and female rats (n = 3–5 per region/sex) using LC-MS. In both sexes, 2-AG was detected at higher concentrations than AEA (nmol/mg tissue versus pmol/mg tissue), in accordance with the findings of others [35] (Fig. 1). Examination of levels of AEA within a sex between brain regions revealed statistical differences (region: $F(1.78, 8.27) = 7.59$, $p = 0.02$). Post-hoc analyses (Tukey) revealed that AEA levels in males (n = 4) were significantly higher in the V1M cortex as compared to PAG ($p = 0.04$ but not Vc ($p = 0.18$) and TG ($p = 0.06$; Fig. 1B); no other statistical differences in AEA levels between regions were detected in males. In female rats, quantification of AEA revealed no differences in levels between brain regions (Tukey post-hoc $p = 0.08$ to 0.97 for all comparisons; Fig. 1B). Between the sexes and within a region, significantly higher amounts of AEA were observed in the V1M cortex such that males had more AEA than females (Sex, n = 3–5/group: $F (1, 6) = 15.95$; $p = 0.007$, Sidak post-hoc, $p = 0.03$; Fig. 1B). No differences in [AEA] in PAG, Vc, or TG were detected between male vs. female rats. Together, region x sex

interaction was statistically significant ($F(3,15) = 193.6$, $p < 0.0001$) suggesting that AEA levels are dependent on sex and region in naïve animals.

Levels of 2AG were determined in V1M cortex, PAG, Vc, and TG from male (n = 4) and female rats (n = 3–5/region) (Fig. 1A). Statistically significant differences in 2AG detection were identified by region ($F(1.98, 15.17) = 91.54$, $p < 0.0001$), sex ($F(1,23 = 56.49$, $p < 0.0001$) and the interaction between ($F(3,23) = 16.2$, $p < 0.0001$). Post-hoc analyses (Tukey) revealed that regional differences in females existed such that PAG > V1M cortex > Vc > TG ($p = < 0.0001$ to 0.42 for all comparisons). In males, PAG showed statistically higher levels of 2AG as compared to TG ($p = 0.03$); no other regional differences were detected in males ($p = 0.09–0.45$; Fig. 1A); no other statistical differences in AEA levels between regions. Between the sexes and within a region, levels of 2AG were statistically higher in female PAG as compared to male PAG (Sidak post-hoc, $p = 0.01$; Fig. 1A). No sex differences were observed in 2AG levels in V1M cortex, Vc, or TG. These data suggest that 2AG levels are dependent on sex and region in naïve animals.

Given the statistical differences in AEA and 2AG levels between the sexes in the V1M cortex and PAG, respectively, as well as regional differences within each sex, subsequent experiments were focused in these regions.

Immunohistochemistry of Endocannabinoid System (ECS) in female and male tissue

In order to examine whether enzymatic differences might underlie the observed sex differences in endocannabinoid tone, we utilized immunohistochemistry to confirm LC-MS findings in the lPAG and V1M cortex (within factor). The lPAG was imaged at high resolution as a locus of the PAG implicated in trigeminal nociception [21–23]. Specifically, these studies evaluated ECS enzyme and receptor immunoreactivity in male and female rats (between factor). Distributions of NAPE-PLD, FAAH, DAGL, MAGL, ABHD6, CB_1R, or CB_2R in neurons, glia, or microglia were evaluated based on colocalization with cell-type specific markers (Nissl for neuronal soma, GFAP for astrocytes and Iba1 for microglia) as a secondary analysis of organizational differences. All analyses were conducted in a region of interest within the V1M cortex and lPAG with statistically similar areas and staining for Nissl, GFAP, and Iba1, Additional Fig. 1)

AEA ECS

NAPE-PLD hydrolyzes NAPE to generate AEA, while degradation of AEA is controlled by FAAH-mediated hydrolysis. Immunohistochemistry was used to test the hypothesis that sex differences in cortical levels of AEA result from variability in the expression and localization of these enzymes (Fig. 2A, B). The interaction between region x sex was statistically significant for FAAH immunoreactivity ($F(1,4) = 41.72$, $p = 0.003$) with the post-hoc analysis revealing a sex difference in the immunoreactivity within the V1M cortex such that male V1M FAAH was detected at higher levels than female (Sidak $p < 0.00001$, Fig. 2E).

No significant differences were observed for the interaction between region x sex in analysis of NAPE-PLD immunoreactivity (Fig. 2C).

To determine whether NAPE-PLD was predominantly in neurons, astocytes or microglia, NAPE-PLD colocalization with Nissl, GFAP, and IBa1 was determined in both sexes for each CNS region (i.e., of all NAPE-PLD, how much co-localized with each marker; Fig. 2D). NAPE-PLD-ir colocalized with Nissl in males significantly more than in females within the V1M cortex ($F(1.15, 4.60) = 144.0$, $p = 0.001$; Sidak post-hoc, $p = 0.004$). No sex differences in colocalization of NAPE-PLD with GFAP or Iba1 in the V1M cortex were observed. Comparison of NAPE-PLD colocalization within the lPAG revealed no significant sex differences between the cell-types (sex: $F(1,4) = 0.12$, $p = 0.74$, Fig. 2D). FAAH-ir colocalization with Nissl, GFAP, and Iba1 was not significantly different between sexes within either region (Fig. 3F).

Finally, in lPAG and V1M cortex, about 50% of NAPE-PLD immunoreactivity did not colocalize with Nissl, GFAP, or Iba1. Similar results were observed with FAAH immunoreactivity. This suggests that both NAPLD-PLD and FAAH are found in additional cellular regions, such as synaptic terminals.

2-AG ECS

2-AG is synthesized from DAGs by DAGL and degraded by serine hydrolases, MAGL and ABHD6. Semi-quantitative immunohistochemistry of these three enzymes was performed to examine the hypothesis that 2-AG levels are higher in female PAG as compared to males as a result of differential enzyme expression, (Fig. 3). DAGL was detected in both male and female samples with higher levels of DAGL found in the female lPAG versus V1M cortex. Similar patterns of overlap with Nissl, GFAP, and Iba1 were observed in both regions for female and male tissue. The interaction between region x sex was statistically significant for DAGL immunoreactivity ($F(1,4) = 21.27$, $p = 0.0099$) with the post-hoc analysis revealing significantly greater immunoreactivity within the female lPAG (Sidak $p = 0.0141$, Fig. 3C).

MAGL immunoreactivity was detected in both male and female tissue within V1M cortex and lPAG (Fig. 3A-B). Statistical analysis revealed female tissue contained significantly greater levels of female MAGL immunoreactivity as compared to males for both regions (sex: $F(1,4) = 195$, $p = 0.0002$; female vs male cortex, Sidak $p = 0.0004$; female vs male lPAG, Sidak $p = 0.0097$). In the lPAG, males showed a significantly higher proportion of MAGL colocalization with Nissl as compared to females ($p = 0.006$, two-way ANOVA). No other significant differences were observed in MAGL colocalization

ABHD6 expression was also detected in the tissue of both sexes (Fig. 3G). Female cortical tissue contained significantly greater levels of ABHD6 immunoreactivity as compared to males within the region (sex: $F(1,4) = 9.703$, $p = 0.0357$; female vs male cortex, Sidak $p = 0.0425$). No significant differences were observed in ABHD6 immunoreactivity within the lPAG. Analysis of co-immunoreactivity showed that ABHD6 overlapped primarily with Nissl in the lPAG; lPAG showed more co-localization of ABHD6 with GFAP than the V1M cortex in the female and male samples (Fig. 3H). In males, ABHD6 co-localized primarily with Nissl in vlPAG.

Overall, the 2-AG-ECS analysis showed that females had higher levels of synthetic DAGL than males in the lPAG, as well as differential expression and localization the degradative enzyme MAGL. Notably, approximately 40–60% of DAGL, MAGL, and ABHD6 immunoreactivity did not colocalize with Nissl, GFAP, or Iba1. These data are suggestive of a sex-based difference in biological and circuit function for the 2-AG-ECS enzyme system within the PAG.

ECS Receptors:

AEA and 2-AG are partial and full agonists at the CBRs, respectively [35] and changes in the levels of these endogenous ligands may be expected to vary with/or alter receptor density. Thus, CB_1R and CB_2R expression levels were compared between the sexes using immunohistochemistry (Fig. 4A, 4B). Analysis of CB_1R immunoreactivity revealed significantly greater staining for CB_1R for females versus males in both the V1M cortex and lPAG (sex: $F(1,4) = 374.7$, $p < 0.0001$; female vs male cortex, Sidak $p < 0.0001$; female vs male lPAG, Sidak $p = 0.001$). CB_2R staining was similarly greater within the female lPAG as compared to the male lPAG. The interaction between region x sex was statistically significant ($F(1,4) = 18.87$, $p = 0.0122$), post-hoc analysis revealed a sex difference in CB_2R staining within the lPAG (Sidak $p = 0.0053$).

Analysis of colocalization revealed that female CB1R immunoreactivity had more overlap overall than male with Nissl, GFAP, or Iba1 independent of CNS region (Female total overlap: ~60%, male total overlap: ~40%, Fig. 4D). Within co-localization, CB_1R showed statistically higher overlap with Nissl in female lPAG and V1M cortex when compared to males ($p = 0.0178$ female lPAG vs male lPAG, two-way ANOVA, $p = 0.008$ female V1M cortex vs male V1M cortex, two-way ANOVA); no differences were seen in the total area for which CB1R overlapped with either GFAP or Iba1 (Fig. 5D). Both males and females showed the highest percentage of overlap of CB_2R with Nissl in the lPAG. No differences were observed in colocalization with GFAP or Iba1 immunoreactivity. Lastly, approximately 40–60% of CB1R and CB2R immunoreactivity did not colocalize with Nissl, GFAP, or Iba1, suggesting location of these receptors on other structures, such as presynaptic terminals. (Fig. 4F).

Proteomic analysis of female and male PAG samples

Seeking to further validate the sex differences observed on IHC and LC-MS, the global proteome between the male and female PAG was examined to identify sex-based patterns in this region relevant to descending pain modulation. The PAG was chosen as the primary focus as LC-MS and IHC studies had identified plausible sex differences in the ECS within this region. Quantitative proteomic analysis comparing global protein expression changes between naïve male and female PAGs identified 6009 total proteins across 72 fractions analyzed for the 6 biological samples (n = 3/sex). A total of 3396 proteins were more prevalent in female PAG with 2449 proteins showing prevalence in males (Fig. 5B, Additional Table 1). Of the 3396 proteins with female prevalence, 512 were present at statistically significantly higher levels than in males, representing 8.5% of all proteins detected (Fig. 5B, Additional Table 1). In

males, 218 proteins were expressed at significantly higher levels as compared to female (3.6% of all proteins detected, Additional Table 2). Unbiased principal component analysis (PCA) of the 730 significantly affected proteins from the two-way ANOVA analysis revealed that the protein expression differences cluster by sex (Fig. 5C; Additional Tables 1–10); 164 proteins showed no sex difference in expression (Additional Table 3). Of these, 595 proteins showed a fold difference of 1.2 or greater (Fig. 5D) with more than 75% being detected at higher levels in females (Fig. 5E, Additional Table 4). Gene ontology (GO) enrichment analysis of the significantly affected proteins using the bioinformatic database DAVID [36, 37] was performed for GO-Molecular Function (MF), GO-Biological Processes (BP), and GO-KEGG pathways (Fig. 5F-H; Additional Tables 5–10). Hydrolase and catalytic activity, lipid metabolism, and metabolic pathways were identified within the top ten significant GO terms in molecular function, biological processes, and KEGG pathways, respectively in females; male terms did not include lipid targeting outcomes.

Individual components of the ECS were assessed in the data set as the GO-BP analysis revealed that regulation of the endocannabinoid system was significantly higher in the female PAG versus male ($P = 0.05$) with a fold enrichment of 38.1. DAGLα, DAGLβ, MAGL, ABHD6, ABHD12, NAPE-PLD 7 isoforms, and CNR1 were detected; neither FAAH nor CNR2 was detected (Table 1). Female PAG contained significantly more MAGL and ABHD6 than males; these were the only differences reaching statistical significance in the ECS data set and showed a 38-fold enrichment as compared to the background gene set in DAVID GO analyses (Additional Tables 1–10). These data, together with the analytical chemistry, suggest that females have a dominance of ECS metabolism in the PAG as compared to males.

Table 1
Sex Differences in PAG ECS Proteome

	Accession	Max fold change over other sex	Anova (p)
Detected Greater in Female	ABHD6_MOUSE*	1.51	0.03
	MGLL_MOUSE*	1.44	0.01
	NAPEP_MOUSE	*1.34*	*0.93*
	PLD3A_MOUSE	1.11	0.46
	PLD2_MOUSE	1.18	0.56
	DGLB_MOUSE	1.05	0.56
	DGLA_RAT;DGLA_MOUSE	*1.01*	*0.85*
Detected Greater in Male	PHLD_MOUSE	1.52	0.15
	PLD1_RAT;PLD1_MOUSE	1.18	0.30
	PLD3_MOUSE	1.07	0.40
	PLD6_MOUSE	1.15	0.84
	CNR1_RAT	*2.49*	*0.13*
	CNRP1_MOUSE;CNRP1_RAT	1.02	0.82
	ABD12_MOUSE	1.02	0.79

Summary of endocannabinoid system (ECS) enzymes detected in greater quantity in either female or male PAG samples, as measured by quantitative proteomics. The 2-AG hydrolyzing enzymes MAGL and ABHD6 (bold) were detected at significantly higher fold-detection for females vs males (ABHD6 female vs. male p = 0.03, MAGL female vs. male p = 0.01). Italics indicates study via IHC. CNR2 and FAAH were below the level of detection in this study.

Protein gene abbreviations: ABHD6- Alpha/Beta-Hydrolase Domain Containing 6; MGLL- Monoacylglycerol Lipase; NAPEP- N-acyl-phosphatidylethanolamine-specific phospholipase D; PLD3A- Phospholipase D3A; PLD2- Phospholipase D2; DGLB- Diacylglycerol lipase beta; DGLA- Diacylglycerol lipase alpha; PHLD-Phosphatidylinositol-Glycan-Specific Phospholipase D; PLD1- Phospholipase D1; PLD3- Phospholipase D3; PLD6- Phospholipase D6; CNR1- Cannabinoid Receptor 1; CNRP1- Cannabinoid Receptor Interacting Protein 1; ABD12- Alpha/Beta-Hydrolase Domain Containing 12

Discussion

The goal of this study was to define the organization of the ECS in neural regions associated with pain in the context of sex. Levels of the primary eCBs, AEA and 2-AG, differed between cortical and brainstem

(i.e., lPAG), but not trigeminal components (Vc or TG), in a sex-dependent manner. Unbiased, quantitative proteomic analysis confirmed sex differences in the PAG proteome such that detection of MAGL and ABHD6 was statistically higher in female than in male samples. Immunohistochemical analysis confirmed the female prevalence of NAPE-PLD, DAGL, and MAGL in the PAG. Moreover, the distribution of CB_1R and CB_2R were significantly different between the sexes as well, with CB_1R lower in males than females in the V1M cortex and PAG. Together, these results suggest differences between the physiology of the male and female ECS in brain regions associated with migraine aura and descending pain modulation. These differences may underscore the sex differences in certain pain etiologies, as well as pharmacological responsivity.

AEA:

Dysregulation of AEA signaling has been implicated in migraine including chronic migraine and medication overuse [39,40], though contested [41]. Peripheral actions of AEA at CB_1R receptors inhibit trigeminal afferent release of neurotransmitters to mitigate headache pain and regulate vascular tone [42]. Levels of AEA are reduced in the plasma of chronic migraine and MOH patients [39]. In addition, female migraineurs, but not male, were reported to have increased activity of AEA transporters and FAAH in platelets, suggesting sex differences [43]. Measurement of AEA in the cerebrospinal fluid revealed that chronic migraineurs and patients with MOH had significantly lower levels as compared to controls or episodic migraineurs [44] suggesting widespread dysfunction of the AEA in the CNS without regional information.

Notably, preclinical study of AEA and its modulation have yielded promising results as a strategy to mitigate migraine. In male rats, following administration of nitroglycerin, an NO-donor used to induce headache pain [45,46], AEA administration blocked changes in expression of TRPV1, NFKb, CRP, and NO [47] and reduced trigeminal activation [48]. Further, FAAH inhibitors were effective as both preventative and reversal agents against NO-induced headache [47,49,50]. Of importance, though NO-induced headache has a reported sexual dimorphism [51], the studies using this model were performed in males [47-50]. Current findings suggest that NAPE-PLD and FAAH are distributed differently amongst neuron, astrocyte, and glial populations as well. These observations combined with clinical reports, indicate that sexual dimorphic responses of restoring physiological AEA tone with FAAH or AMT inhibitors warrant additional investigation with attention to female subjects [52].

Our data support sex differences in the levels of AEA in the V1M cortex, but not PAG. As the above studies have demonstrated the anti-migraine effects of AEA, this may offer males increased protection against trigeminal nociception.

2-AG:

The role of 2-AG has been understudied in migraine and pain states. Clinically, levels of 2-AG in platelets of chronic migraineurs and MOH patients were lower than controls subjects [53]. However, CSF levels were below the limit of detection in other studies [43,44]. 2-AG acts on both cannabinoid receptors, leading to reduction in neurotransmitter release at glutamatergic and GABA-ergic synapses [11-15]. Thus, alterations in levels of 2-AG are pertinent to pain sensation in the V1M cortex and descending pain modulation in the PAG and V1M cortex.

Our results show that 2-AG levels are significantly higher in the female PAG as compared to male PAG and V1M cortex. Thus, investigations of platelets or CSF in headache patients may not reflect important differences within discrete brain circuits relevant to pain transmission. Given the differences in PAG 2-AG levels between male and female rats and clinical inconsistencies in reporting of 2-AG levels, it is possible that sex differences in the expression or activity of synthetic (DAGL) or degradative enzymes (MAGL, ABHD6) for 2-AG underlie the observed sex difference in 2-AG levels.

DAGL:

Preclinically, DAGLα expression is reported in the perisynaptic region of the dendritic spines of glutamatergic synapses [54], although cytosolic and nuclear DAGLα are also described in cortical neurons [55]. Studies above observed DAGLα in neuronal soma and fibers, astrocytes, and microglia in both the V1M cortex and PAG. Recently, mutations in DAGLA, the gene for DAGLα, within the CNS, were identified and implicated in neurological disorders in humans [56]. Furthermore, there is evidence that depletion of 2-AG via inhibition of DAGLα may be sufficient to trigger migraine-like pain in animals [57]. Thus, pathological reductions in the functional expression of DAGLα in females during pain states, including headache, may have a pronounced impact via decreased 2-AG signaling.

Our studies revealed that DAGLα expression was higher in female rat PAG as compared to male using immunofluorescence; similar patterns were observed in the V1M cortex. The significantly greater amount of DAGLα detected in the female PAG offers one explanation for the greater levels of 2-AG observed in this region; however, sex differences in the levels of 2-AG hydrolyzing enzymes must be considered as well.

MAGL and ABHD6:

In contrast to increases in DAGL synthesis of 2-AG, higher levels of 2-AG in female PAG may reflect lower expression of functional degradative enzymes, MAGL and ABHD6. Both MAGL and ABHD6 degrade many monoacylglycerol species, including 2-AG [7,8,58-62]. MAGL and ABHD6 inhibitors have shown promise as pain therapeutics [57, 62-66] and in treating neurological disorders [7,8,62], respectively. One study investigated the contribution of MAGL to NO-induced headache, but results were not obtained in both sexes [50]. Mechanistically, the effect of the inhibitors has correlated to increasing 2-AG levels and CBR signaling while attenuating eicosanoid signaling [12,68].

Present proteomic and immunohistochemical data indicate that 2-AG degradation may be higher in females as compared to males in the PAG. Notably, ABHD6 has been shown to have DAGL activity in addition to the breakdown of monoacylglycerols [69], and this may contribute to the sex differences in 2-AG levels within PAG. Our findings suggest that sex differences in the prevalence of disorders where the PAG is implicated, including migraine and other pain states, [70-78], may result from inherent differences in synthesis and degradation of 2-AG. Sex differences in signaling of 2-AG at the eCB receptors within pain modulatory pathways may influence the frequency and intensity of pain signals sent to the somatosensory cortex.

CB Receptors:

In the context of pain, preclinical data support sex differences in responsivity to cannabinoid receptor agonists including Δ^9-tetrahydrocannabinol (THC), cannabidiol, beta-caryophyllene (BCP), WIN55-212-2, and CP55-940 [78-81]. In support of the theory of CED, Kandasamy et al. demonstrated THC, a $CB_{1/2}$ agonist, ameliorated the effects of induced migraine in rats, and that this effect was attenuated on administration of a CB_1 antagonist [79]. CB_2R expression in the CNS has been controversial, and current clinical literature supports a role for it during inflammation [35,83-86].

Agonism of the CB receptors is being pursued for several neurological disorders, including migraine [6,86-91]. In addition, more than 300 publications report sex differences in pathologies where the ECS plays a regulatory role. Our data now reveal that these sex differences are discernable in discrete brain regions and cell types within pain relevant regions of the CNS. Thus, cannabinoid pharmacology may have anatomical and circuit-based differences between the sexes in basal and pathological states.

Female cortical and lPAG sections showed significantly higher CB_1R immunoreactivity as compared to the respective male tissue. Male CB_2R expression was largely in neurons, whereas female colocalization was primarily in glial cells. These data suggest that differences in the literature reporting CNS expression of CB_2R would benefit from analysis by sex and that CB_2R in the CNS may play different roles between male and female subjects. Given the interest in developing CB_2R targeting therapeutics for pain and neurological disorders, these sex differences in the biological role of CB_2R are important [92,93].

ECS distribution in Neurons, Glia, and Immune Cells:

Throughout the immunohistochemical analyses, it was observed that for all proteins in the ECS, colocalization with Nissl (neuronal soma), GFAP (astrocyte marker), and Iba1 (microglial marker) was limited to 40-70%. Thus, 30-60% of the ECS proteins were observed independent of these markers. It is possible that a portion of the observed proteins that were non-localized were due to aberrant pixel detection, either from background noise on the image or from image artifacts. However, there is evidence within the literature for the role of these proteins at synaptic terminals, which may have eluded the

selected cell markers [6-8,38]. Proteins present in the neurovasculature and extracellular spaces likely would not be co-localized with our cellular markers. For all immunohistochemical analyses, the overall staining/immunoreactivity with these biomarkers of cellular identity (neuron, astrocyte, or microglia) were the same between regions and each sex, confirming that regional comparisons were appropriately controlled for cell types and number (Additional Fig 1).

Limitations:

Though carefully designed, this study does have some limitations. First, immunohistochemistry with antibodies targeting proteins of interest was used. Antibodies, particularly those against the cannabinoid receptors, are reported to be non-specific and unreliable [94,95]. To combat this, we paired imaging with an unbiased quantitative proteomics approach. This unbiased method allowed for determining presence of proteins in each region by sex, but itself is limited in spatial resolution by cell type. This lack of detection may reflect masking by proteins with higher abundance (i.e. low signal to noise). Second, all tissue was obtained from Sprague-Dawley rats between 7-8 weeks old. As the ECS is implicated in neural development [96,97], it is possible that sex differences identified here become more/less prominent during aging. Finally, endocannabinoid levels were obtained from uncycled female animals. Several reports indicate that both 2-AG and AEA levels change with the estrus cycle including in the brain [80,98]. Therefore, sex differences noted here of ECS functional expression may fluctuate in magnitude across the estrus cycle. Future studies should incorporate newly developed fluorescent chemical probes for labeling these CBRs to confirm the present observations [99,100] and investigate the sex difference in the ECS with aging and in cycled females.

Perspectives And Significance

Neuropathological disorders such as chronic pain, migraine, and multiple sclerosis are associated with a large sex difference in prevalence. Moreover, the pharmacology of analgesics, including cannabinoids, is documented as having sex selective outcomes. Our observations suggest that sex differences exist with regional and cellular selectivity in the neuroanatomical arrangement of the ECS within the V1M cortex and PAG. The V1M cortex, a locus of pain sensation and modulation, showed the greatest amount of AEA in males. If AEA signaling at cortical CB_1R and CB_2R is primarily inhibitory, this may offer males greater protection against pain sensation and migraine-associated cortical spreading depression than females. 2-AG, along with its synthesizing and degrative enzymes, was detected highest in female PAG. As the PAG participates in descending pain modulation, alterations to 2-AG levels may be more relevant during pain in females. This sexual dimorphism of the ECS within pain modulatory pathways may underscore the sex differences observed in pain etiologies and cannabis pharmacology and indicates that both pain and pharmacological investigations should take sex into account when studying the ECS.

Declarations

Ethics Approval

All animal procedures were performed during the 12-hour light cycle and according to the policies and recommendations of the International Association for the Study of Pain, the NIH guidelines for laboratory animals, with IACUC approval from the University of Arizona.

Consent for Publication

Not Applicable

Availability of Data and Materials

The datasets used and/or analyzed during the current study are available from the corresponding author on reasonable request.

Competing Interests

The Authors report no conflicts of interest.

Funding

This work was supported by grants from the National Institute of Neurological Disorders and Stroke (R01NS099292, TML) of the National Institutes of Health, Arizona Biomedical Research Commission (ABRC45952, TML), with monies from the Department of Pharmacology at the University of Arizona, the M.D.-Ph.D. Program at the University of Arizona, and the University of Arizona Comprehensive Pain and Addiction Center. Research reported in this publication was also supported by the National Cancer Institute of the National Institutes of Health under award number P30 CA023074. Authors are solely responsible for the content which does not necessarily represent the official views of the National Institutes of Health, the State of Arizona, or the University of Arizona.

Author’s Contributions

Aidan Levine: Experimental design, data collection/analysis, manuscript preparation

Erika Liktor-Busa: Experimental design, data collection/analysis/ and interpretation, manuscript preparation

Austin A. Lipinski: Data collection/analysis

Sarah Cotoure: Data collection/analysis

Shreya Balasubramanian: Data collection/analysis

Sue A. Aicher: Data interpretation/Manuscript preparation

Paul R. Langlais: Data collection/analysis/ and interpretation, manuscript preparation

Todd W. Vanderah: Experimental design and manuscript preparation

Tally M. Largent-Milnes: Experimental design, data analysis/interpretation, manuscript preparation

Acknowledgements

The authors would like to acknowledge the assistance of Douglas Cromey, MS, manager for optical microscopes in the Imaging Cores-Life Sciences North. The Zeiss Elyra S.1 Microscope is part of the Imaging Cores-Life Sciences North, which is overseen by the University of Arizona Research Labs (purchase supported by NIH S10 OD019948). University of Arizona Cancer Center's Analytical Chemistry Shared Resources is acknowledged for the assistance of LC-MS service. The authors acknowledge the assistance of Dean Billheimer, Ph.D., director of the UA Statistical Consulting lab, for statistical analysis and confirming appropriateness of statistical tests used for the data.

References

1. Dahlhamer J, Lucas J, Zelaya C, Nahin R, Mackey S, DeBar L, et al. Prevalence of Chronic Pain and High-Impact Chronic Pain Among Adults - United States, 2016. Morb Mortal Wkly Rep. 2018;67:1001–6.
2. Sparks JA. Rheumatoid Arthritis. Ann Intern Med. 2019;170:ITC1–16.
3. Russo EB. Clinical Endocannabinoid Deficiency Reconsidered: Current Research Supports the Theory in Migraine, Fibromyalgia, Irritable Bowel, and Other Treatment-Resistant Syndromes. Cannabis Cannabinoid Res. 2016;1:154–65.
4. Ahn K, McKinney MK, Cravatt BF. Enzymatic pathways that regulate endocannabinoid signaling in the nervous system. Chem Rev. 2008;108:1687–707.
5. Fezza F, Mastrangelo N, Maccarrone M. Assay of NAPE-PLD Activity. Methods Mol Biol. 2016;1412:123–30.
6. Murataeva N, Straiker A, Mackie K. Parsing the players: 2-arachidonoylglycerol synthesis and degradation in the CNS. Br J Pharmacol. 2014;171:1379–91.
7. Cao JK, Kaplan J, Stella N. ABHD6: Its Place in Endocannabinoid Signaling and Beyond. Trends Pharmacol Sci. 2019;40:267–77.

8. Marrs WR, Blankman JL, Horne EA, Thomazeau A, Lin YH, Coy J, et al. The serine hydrolase ABHD6 controls the accumulation and efficacy of 2-AG at cannabinoid receptors. Nat Neurosci. 2010;13:951–7.
9. Savinainen JR, Saario SM, Laitinen JT. The serine hydrolases MAGL, ABHD6 and ABHD12 as guardians of 2-arachidonoylglycerol signaling through cannabinoid receptors. Acta Physiol (Oxf). 2012;204:267–76.
10. Turcotte C, Blanchet MR, Laviolette M, Flamand N. The CB2 receptor and its role as a regulator of inflammation. Cell Mol Life Sci. 2016;73:4449–70.
11. Davis MP. Cannabinoids in pain management: CB1, CB2 and non-classic receptor ligands. Expert Opin Investig Drugs. 2014;23:1123–40.
12. Nomura DK, Morrison BE, Blankman JL, Long JZ, Kinsey SG, Marcondes MC, et al. Endocannabinoid hydrolysis generates brain prostaglandins that promote neuroinflammation. Science. 2011;334:809–13.
13. Quartilho A, Mata HP, Ibrahim MM, Vanderah TW, Porreca F, Makriyannis A, Malan TP Jr. Inhibition of inflammatory hyperalgesia by activation of peripheral CB2 cannabinoid receptors. Anesthesiology. 2003;99:955–60.
14. Sanchez-Blazquez P, Rodriguez-Munoz M, Garzon J. The cannabinoid receptor 1 associates with NMDA receptors to produce glutamatergic hypofunction: implications in psychosis and schizophrenia. Front Pharmacol. 2014;4:169.
15. Tumati S, Largent-Milnes TM, Keresztes A, Ren J, Roeske WR, Vanderah TW, Varga EV. Repeated morphine treatment-mediated hyperalgesia, allodynia and spinal glial activation are blocked by co-administration of a selective cannabinoid receptor type-2 agonist. J Neuroimmunol. 2012;244:23–31.
16. Dodick DW. A Phase-by-Phase Review of Migraine Pathophysiology. Headache. 2018;58:4–16.
17. Malick A, Strassman RM, Burstein R. Trigeminohypothalamic and reticulohypothalamic tract neurons in the upper cervical spinal cord and caudal medulla of the rat. J Neurophysiol. 2000;84:2078–112.
18. Pietrobon D, Moskowitz MA. Pathophysiology of migraine. Annu Rev Physiol. 2013;75:365–91.
19. Lu C, Yang T, Zhao H, Zhang M, Meng F, Fu H, Xie Y, Xu H. Insular Cortex is Critical for the Perception, Modulation, and Chronification of Pain. Neurosci Bull. 2016;32(2):191–201.
20. Ong W, Stohler CS, Herr DR. Role of the Prefrontal Cortex in Pain Processing. Mol Neruobiol. 2019;56:1137–66.
21. Morgan MM, Whittier KL, Hegarty DM, Aicher SA. Periaqueductal gray neurons project to spinally projecting GABAergic neurons in the rostral ventromedial medulla. Pain. 2008;140:376–86.
22. Kong J, Tu P, Zyloney C, Su T. Intrinsic functional connectivity of the periaqueductal gray, a resting fMRI study. Behav Brain Res. 2010;211:215–9.
23. Aicher SA, Hermes SM, Whittier KL, Hegarty DM. Descending projections from the rostral ventromedial medulla (RVM) to trigeminal and spinal dorsal horns are morphologically and

neurochemically distinct. J Chem Neuroanat. 2012;43:103–11.

24. Smitherman TA, Burch R, Sheikh H, Loder E. The prevalence, impact, and treatment of migraine and severe headaches in the United States: a review of statistics from national surveillance studies. Headache. 2013;53:427–36.
25. Yunus MB. Gender differences in fibromyalgia and other related syndromes. J Gend Specif Med. 2002;5:42–7.
26. Andrews NA, Latrémolière A, Basbaum AI, Mogil JS, Porreca F, Rice AS, et al. Ensuring transparency and minimization of methodologic bias in preclinical pain research: Precise considerations. Pain. 2016;157:901–9.
27. Schindelin J, Arganda-Carreras I, Friese E, et al. Fiji: an open-source platform for biological image analysis. Nature Method. 2012;9(7):676–82.
28. Crowe AR, Yue W. Semi-Quantitiative Determination of Protein Expression Using Immunohistochemistry Staining and Analysis: An Integrated Protocol. Bio Protoc. 2019;9(24):e3465.
29. Model M, Burkhardt J. A standard for calibration and correction of a fluorescence microscope. J Quant Cell Sci. 2001;44(4):309–16.
30. Wilkerson JL, Niphakis MJ, Grim TW, Mustafa MA, Abdullah RA, Poklis JL, et al. The Selective Monoacylglycerol Lipase Inhibitor MJN110 Produces Opioid-Sparing Effects in a Mouse Neuropathic Pain Model. J Pharmacol Exp Ther. 2016;357:145–56.
31. Kruse R, Krantz J, Barker N, Coletta RL, Rafikov R, Luo M, et al. Characterization of the CLASP2 Protein Interaction Network Identifies SOGA1 as a Microtubule-Associated Protein. Mol Cell Proteomics. 2017;16:1718–35.
32. Parker SS, Krantz J, Kwak EA, Barker NK, Deer CG, Lee NY, et al. Insulin Induces Microtubule Stabilization and Regulates the Microtubule Plus-end Tracking Protein Network in Adipocytes. Mol Cell Proteomics. 2019;18:1363–81.
33. Tyanova S, Cox J. Perseus. A Bioinformatics Platform for Integrative Analysis of Proteomics Data in Cancer Research. Methods Mol Biol. 2018;1711:133–48.
34. Tyanova S, Temu T, Sinitcyn P, Carlson A, Hein MY, Geiger T, et al. The Perseus computational platform for comprehensive analysis of (prote)omics data. Nat Methods. 2016;13:731–40.
35. Zou S, Kumar U. Cannabinoid Receptors and the Endocannabinoid System: Signaling and Function in the Central Nervous System. Int J Mol Sci. 2018;19:833.
36. Huang da W, Sherman BT, Lempicki RA. Bioinformatics enrichment tools: paths toward the comprehensive functional analysis of large gene lists. Nucleic Acids Res. 2009;37:1–13.
37. Huang da W, Sherman BT, Lempicki RA. Systematic and integrative analysis of large gene lists using DAVID bioinformatics resources. Nat Protoc. 2009;4:44–57.
38. Hu SS, Mackie K. Distribution of the Endocannabinoid System in the Central Nervous System. Handb Exp Pharmacol. 2015;231:59–93.

39. Cupini LM, Costa C, Sarchielli P, Bari M, Battista N, Eusebi P, et al. Degradation of endocannabinoids in chronic migraine and medication overuse headache. Neurobiol Dis. 2008;30:186–9.
40. Perrotta A, Arce-Leal N, Tassorelli C, Gasperi V, Sances G, Blandini F, et al. Acute reduction of anandamide-hydrolase (FAAH) activity is coupled with a reduction of nociceptive pathways facilitation in medication-overuse headache subjects after withdrawal treatment. Headache. 2012;52:1350–61.
41. Gouveia-Figueira S, Goldin K, Hashemian SA, Lindberg A, Persson M, Nording ML, et al. Plasma levels of the endocannabinoid anandamide, related N-acylethanolamines and linoleic acid-derived oxylipins in patients with migraine. Prostaglandins Leukot Essent Fatty Acids. 2017;120:15–24.
42. Akerman S, Kaube H, Goadsby PJ. Anandamide is able to inhibit trigeminal neurons using an in vivo model of trigeminovascular-mediated nociception. J Pharmacol Exp Ther. 2004;309:56–63.
43. Cupini LM, Bari M, Battista N, Argirò G, Finazzi-Agrò A, Calabresi P, et al. Biochemical changes in endocannabinoid system are expressed in platelets of female but not male migraineurs. Cephalalgia. 2006;26:277–81.
44. Sarchielli P, Pini LA, Coppola F, Rossi C, Baldi A, Mancini ML, et al. Endocannabinoids in chronic migraine: CSF findings suggest a system failure. Neuropsychopharmacology. 2007;32:1384–90.
45. Pradhan AA, Smith ML, McGuire B, Tarash I, Evans CJ, Charles A. Characterization of a novel model of chronic migraine. Pain. 2014;155:269–74.
46. Pradhan AA, Smith ML, Zyuzin J, Charles A. δ-Opioid receptor agonists inhibit migraine-related hyperalgesia, aversive state and cortical spreading depression in mice. Br J Pharmacol. 2014;171:2375–84.
47. Nagy-Grócz G, Tar L, Bohár Z, Fejes-Szabó A, Laborc KF, Spekker E, et al. The modulatory effect of anandamide on nitroglycerin-induced sensitization in the trigeminal system of the rat. Cephalalgia. 2016;36:849–61.
48. Greco R, Mangione AS, Sandrini G, Maccarrone M, Nappi G, Tassorelli C. Effects of anandamide in migraine: data from an animal model. J Headache Pain. 2011;12:177–83.
49. Greco R, Demartini C, Zanaboni AM, Tumelero E, Reggiani A, Misto A, et al. FAAH inhibition as a preventive treatment for migraine: A pre-clinical study. Neurobiol Dis. 2020;134:104624.
50. Nozaki C, Markert A, Zimmer A. Inhibition of FAAH reduces nitroglycerin-induced migraine-like pain and trigeminal neuronal hyperactivity in mice. Eur Neuropsychopharmacol. 2015;25:1388–96.
51. Greco R, Tassorelli C, Mangione AS, Smeraldi A, Allena M, Sandrini G, et al. Effect of sex and estrogens on neuronal activation in an animal model of migraine. Headache. 2013;53:288–96.
52. McPartland JM, Guy GW, Di Marzo V. Care and feeding of the endocannabinoid system: a systematic review of potential clinical interventions that upregulate the endocannabinoid system. PLoS One. 2014;9:e89566.
53. Rossi C, Pini LA, Cupini ML, Calabresi P, Sarchielli P. Endocannabinoids in platelets of chronic migraine patients and medication-overuse headache patients: relation with serotonin levels. Eur J Clin Pharmacol. 2008;64:1–8.

54. Yoshida T, Fukaya M, Uchigashima M, Miura E, Kamiya H, Kano M, et al. Localization of diacylglycerol lipase-alpha around postsynaptic spine suggests close proximity between production site of an endocannabinoid, 2-arachidonoyl-glycerol, and presynaptic cannabinoid CB1 receptor. J Neurosci. 2006;26:4740–51.
55. García del Caño G, Montaña M, Aretxabala X, González-Burguera I, López de Jesús M, Barrondo S, et al. Nuclear phospholipase C-β1 and diacylglycerol LIPASE-α in brain cortical neurons. Adv Biol Regul. 2014;54:12–23.
56. Smith DR, Stanley CM, Foss T, Boles RG, McKernan K. Rare genetic variants in the endocannabinoid system genes CNR1 and DAGLA are associated with neurological phenotypes in humans. PLoS One. 2017;12:e0187926.
57. Levine A, Liktor-Busa E, Karlage KL, Giancotti L, Salvemini D, Vanderah TW, Largent-Milnes TM. DAGLα Inhibition as a Non-invasive and Translational Model of Episodic Headache. Front Pharmacol. 2021;11:615028.
58. Long JZ, Nomura DK, Cravatt BF. Characterization of monoacylglycerol lipase inhibition reveals differences in central and peripheral endocannabinoid metabolism. Chem Biol. 2009;16:744–53.
59. Nomura DK, Long JZ, Niessen S, Hoover HS, Ng SW, Cravatt BF. Monoacylglycerol lipase regulates a fatty acid network that promotes cancer pathogenesis. Cell. 2010;140:49–61.
60. Nomura DK, Lombardi DP, Chang JW, Niessen S, Ward AM, Long JZ, et al. Monoacylglycerol lipase exerts dual control over endocannabinoid and fatty acid pathways to support prostate cancer. Chem Biol. 2011;18:846–56.
61. Savinainen JR, Kansanen E, Pantsar T, Navia-Paldanius D, Parkkari T, Lehtonen M, et al. Robust hydrolysis of prostaglandin glycerol esters by human monoacylglycerol lipase (MAGL). Mol Pharmacol. 2014;86:522–35.
62. Shields CM, Zvonok N, Zvonok A, Makriyannis A. Biochemical and Proteomic Characterization of Recombinant Human α/β Hydrolase Domain 6. Sci Rep. 2019;9:890.
63. Comelli F, Giagnoni G, Bettoni I, Colleoni M, Costa B. The inhibition of monoacylglycerol lipase by URB602 showed an anti-inflammatory and anti-nociceptive effect in a murine model of acute inflammation. Br J Pharmacol. 2017;152:787–94.
64. Kinsey SG, Long JZ, O'Neal ST, Abdullah RA, Poklis JL, Boger DL, et al. Blockade of endocannabinoid-degrading enzymes attenuates neuropathic pain. J Pharmacol Exp Ther. 2009;330:902–10.
65. Kinsey SG, Long JZ, Cravatt BF, Lichtman AH. Fatty acid amide hydrolase and monoacylglycerol lipase inhibitors produce anti-allodynic effects in mice through distinct cannabinoid receptor mechanisms. J Pain. 2010;11:1420–8.
66. Kinsey SG, Nomura DK, O'Neal ST, Long JZ, Mahadevan A, Cravatt BF, et al. Inhibition of monoacylglycerol lipase attenuates nonsteroidal anti-inflammatory drug-induced gastric hemorrhages in mice. J Pharmacol Exp Ther. 2011;338:795–802.

67. Thompson AL, Grenald SA, Ciccone H, Neemah B, Staatz WD, Niphakis MJ, et al. The Endocannabinoid System Alleviates Pain in a Murine Model of Cancer-Induced Bone Pain. J Pharmacol Exp Ther. 2020;373:230–8.
68. Nomura DK, Hudak CS, Ward AM, Burston JJ, Issa RS, Fisher KJ, et al. Monoacylglycerol lipase regulates 2-arachidonoylglycerol action and arachidonic acid levels. Bioorg Med Chem Lett. 2008;18:5875–8.
69. van Esbroeck ACM, Kantae V, Di X, van der Wel T, den Dulk H, Stevens AF, et al. Identification of α,β-Hydrolase Domain Containing Protein 6 as a Diacylglycerol Lipase in Neuro-2a Cells. Front Mol Neurosci. 2019;12:286.
70. Boes T, Levy D. Influence of sex, estrous cycle, and estrogen on intracranial dural mast cells. Cephalalgia. 2012;32:924–31.
71. Borsook D, Erpelding N, Lebel A, Linnman C, Veggeberg R, Grant PE, et al. Sex and the migraine brain. Neurobiol Dis. 2014;68:200–14.
72. Burch RC, Loder S, Loder E, Smitherman TA. The prevalence and burden of migraine and severe headache in the United States: updated statistics from government health surveillance studies. Headache. 2015;55:21–34.
73. Chai NC, Peterlin BL, Calhoun AH. Migraine and estrogen. Curr Opin Neurol. 2014;27:315–24.
74. Faria V, Erpelding N, Lebel A, Johnson A, Wolff R, Fair D, et al. The migraine brain in transition: girls vs boys. Pain. 2015;156:2212–21.
75. Martella G, Costa C, Pisani A, Cupini LM, Bernardi G, Calabresi P. Antiepileptic drugs on calcium currents recorded from cortical and PAG neurons: therapeutic implications for migraine. Cephalalgia. 2008;28:1315–26.
76. Martin VT, Pavlovic J, Fanning KM, Buse DC, Reed ML, Lipton RB. Perimenopause and Menopause Are Associated With High Frequency Headache in Women With Migraine: Results of the American Migraine Prevalence and Prevention Study. Headache. 2016;56:292–305.
77. Rasmussen BK, Olesen J. Migraine with aura and migraine without aura: an epidemiological study. Cephalalgia. 1992;12:221–8.
78. Russell MB, Rasmussen BK, Thorvaldsen P, Olesen J. Prevalence and sex-ratio of the subtypes of migraine. Int J Epidemiol. 1995;24:612–8.
79. Kandasamy R, Dawson CT, Craft RM, Morgan MM. Anti-migraine effect of Δ9-tetrahydrocannabinol in the female rat. Eur J Pharmacol. 2018;818:271–7.
80. Bradshaw HB, Rimmerman N, Krey JF, Walker JM. Sex and hormonal cycle differences in rat brain levels of pain-related cannabimimetic lipid mediators. Am J Physiol Regul Integr Comp Physiol. 2006;291:R349–58.
81. Ceccarelli I, Fiorenzani P, Pessina F, Pinassi J, Aglianò M, Miragliotta V, et al. The CB2 Agonist β-Caryophyllene in Male and Female Rats Exposed to a Model of Persistent Inflammatory Pain. Front Neurosci. 2020;14:850.

82. Cooper ZD, Craft RM. Sex-Dependent Effects of Cannabis and Cannabinoids: A Translational Perspective. Neuropsychopharmacology. 2018;43:34–51.
83. Bie B, Wu J, Foss JF, Naguib M. An overview of the cannabinoid type 2 receptor system and its therapeutic potential. Curr Opin Anaesthesiol. 2018;31:407–14.
84. Chen DJ, Gao M, Gao FF, Su QX, Wu J. Brain cannabinoid receptor 2: expression, function and modulation. Acta Pharmacol Sin. 2017;38:312–6.
85. Ni R, Mu L, Ametamey S. Positron emission tomography of type 2 cannabinoid receptors for detecting inflammation in the central nervous system. Acta Pharmacol Sin. 2019;40:351–7.
86. Burston JJ, Woodhams SG. Endocannabinoid system and pain: an introduction. Proc Nutr Soc. 2014;73:106–17.
87. Cahill K, Ussher M. Cannabinoid type 1 receptor antagonists (rimonabant) for smoking cessation. Cochrane Database Syst Rev. 2007;3:CD005353.
88. Rahn EJ, Hohmann AG. Cannabinoids as pharmacotherapies for neuropathic pain: from the bench to the bedside. Neurotherapeutics. 2009;6:713–37.
89. Santos PS, Oliveira TC, Júnior R, Figueiras LM, Nunes A. LCC. β-caryophyllene Delivery Systems: Enhancing the Oral Pharmacokinetic and Stability. Curr Pharm Des. 2018;24:3440–53.
90. Wiley JL, Marusich JA, Huffman JW. Moving around the molecule: relationship between chemical structure and in vivo activity of synthetic cannabinoids. Life Sci. 2014;97:55–63.
91. Lozano-Ondoua AN, Hanlon KE, Symons-Liguori AM, Largent-Milnes TM, Havelin JJ, Ferland HL III, et al. Disease Modification of Breast Cancer-induced Bone Remodeling by Cannabinoid CB2 receptor Agonists. J Bone Miner Res. 2013;28:92–107.
92. Dhopeshwarkar A, Mackie K. CB2 Cannabinoid receptors as a therapeutic target-what does the future hold? Mol Pharmacol. 2014;86:430–7.
93. Navarro G, Morales P, Rodríguez-Cueto C, Fernández-Ruiz J, Jagerovic N, Franco R. Targeting Cannabinoid CB2 Receptors in the Central Nervous System. Medicinal Chemistry Approaches with Focus on Neurodegenerative Disorders. Front Neurosci. 2016;10:406.
94. Marchalant Y, Brownjohn PW, Bonnet A, Kleffmann T, Ashton JC. Validating Antibodies to the Cannabinoid CB2 Receptor: Antibody Sensitivity Is Not Evidence of Antibody Specificity. J Histochem Cytochem. 2014;62:395–404.
95. Pacher P, Kunos G. Modulating the endocannabinoid system in human health and disease–successes and failures. FEBS J. 2013;280:1918–43.
96. Meyer HC, Lee FS, Gee DG. The Role of the Endocannabinoid System and Genetic Variation in Adolescent Brain Development. Neuropsychopharmacology. 2018;43:21–33.
97. Skaper SD, Di Marzo V. Endocannabinoids in nervous system health and disease: the big picture in a nutshell. Philos Trans R Soc Lond B Biol Sci. 2012;367:3193–200.
98. Walker OS, Holloway AC, Raha S. The role of the endocannabinoid system in female reproductive tissues. J Ovarian Res. 2019;12:3.

99. Soethoudt M, Stolze SC, Westphal MV, van Stralen L, Martella A, van Rooden EJ, et al. Selective Photoaffinity Probe That Enables Assessment of Cannabinoid CB2 Receptor Expression and Ligand Engagement in Human Cells. J Am Chem Soc. 2018;140:6067–75.
100. Westphal MV, Sarott RC, Zirwes EA, Osterwald A, Guba W, Ullmer C, et al. Highly Selective, Amine-Derived Cannabinoid Receptor 2 Probes. Chemistry. 2020;26:1380–7.

Figures

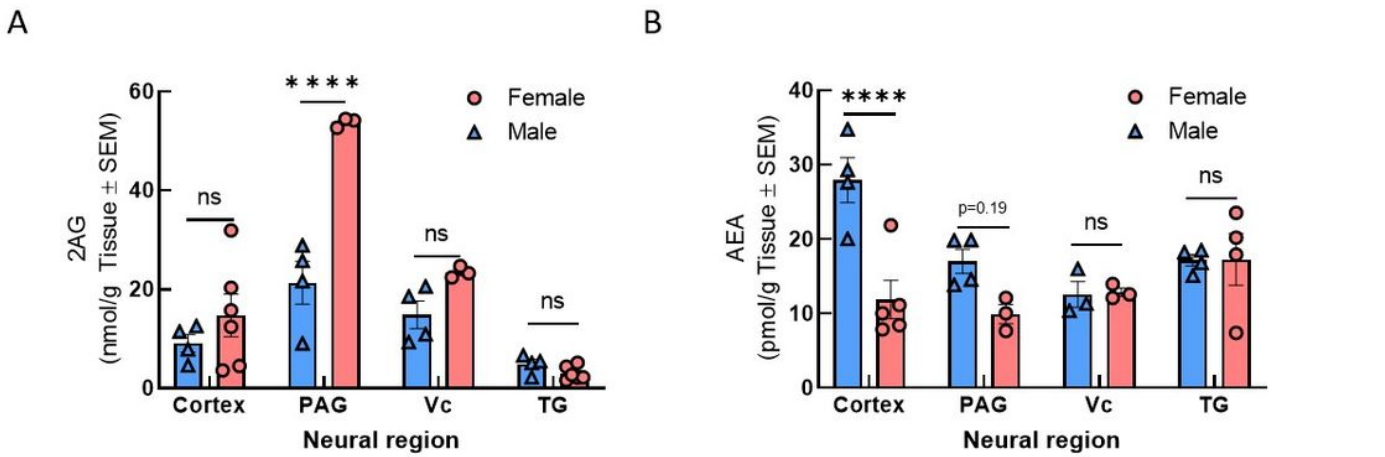

Figure 1

Figure 1

Regional and sex-differences in the level of two main endocannabinoids, 2AG and AEA. Regional and sex-differences of 2-AG (A) and AEA (B) level were observed in CNS areas (V1M cortex, PAG, Vc, and TG) harvested from naïve female and male SD rats. (A) Significantly reduced level of 2AG was measured in female V1M cortex, Vc, and TG areas compared to PAG (#### p<0.0001 vs. female PAG). Regional differences of 2AG level were identified in male PAG vs. male TG (#p=0.01, male PAG vs. male TG). Sex-differences of 2AG level was noticed in PAG samples (****p<0.0001, male PAG vs. female PAG). (B) There were no significant differences in the level of AEA in female samples, but AEA concentration was significantly lower in male PAG, Vc, and TG compared to male V1M cortex (#p=0.04, # # p=0.0045, vs. V1M cortex). Sex-differences of AEA level was detected in V1M cortex samples (***p=0.0006, male V1M cortex vs. female V1M cortex). Values are the mean ± SEM (n=3-6). Statistical analysis was assessed by one-way ANOVA. n.s.= non-significant.

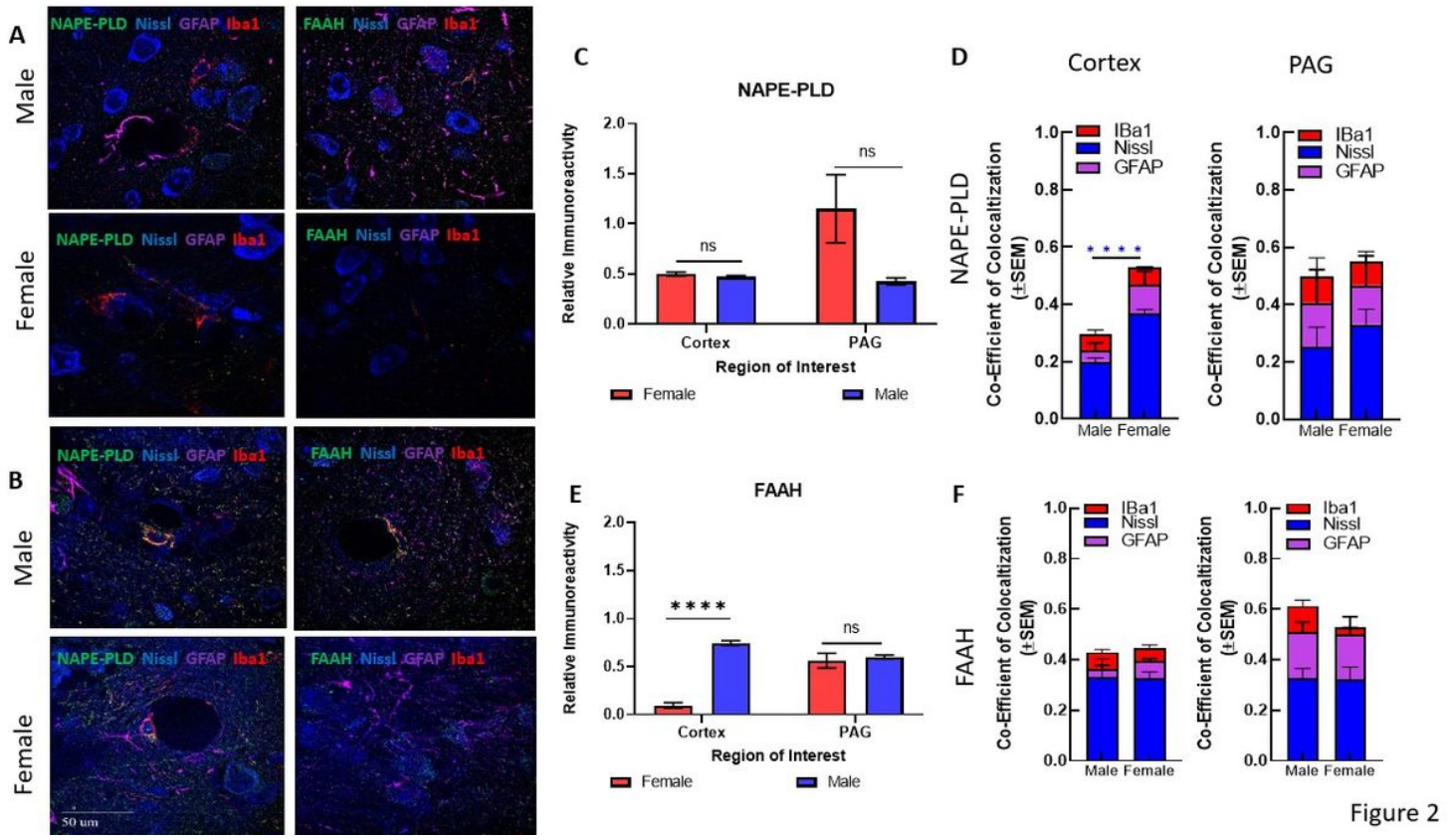

Figure 2

Figure 2

Immunohistochemical Analysis of the AEA System (A) Immunohistochemistry of naïve male and female cortex. Staining for NAPE-PLD, FAAH, Iba1, GFAP, and Nissl was performed. Original magnification 63X. (B) Immunohistochemistry of naïve male and female PAG. Staining for NAPE-PLD, FAAH, Iba1, GFAP, and Nissl was performed. Original magnification 63X. . Scale on lower left image applies to all frames (C) Measurement of relative area of IHC field occupied by NAPE-PLD staining pixels for each sex and region. No significant differences were observed between region or sex (D) Measurement of co-efficient of colocalization for NAPE-PLD with IBa1, Nissl, and GFAP. NAPE-PLD colocalized with Nissl at significantly higher rates in Female cortex vs male cortex (****p=0.004). No significant differences observed in PAG. (E) Measurement of relative area of IHC field occupied by FAAH staining pixels for each sex and region. FAAH immunoreactivity was significantly higher in Male cortex vs Female Cortex (****p=0.003) (F) Measurement of co-efficient of colocalization for FAAH with IBa1, Nissl, and GFAP. No significant differences observed between region or sex. All calculations for co-efficient of colocalization were performed with respect to the relevant enzyme. N=3/sex for each analysis.

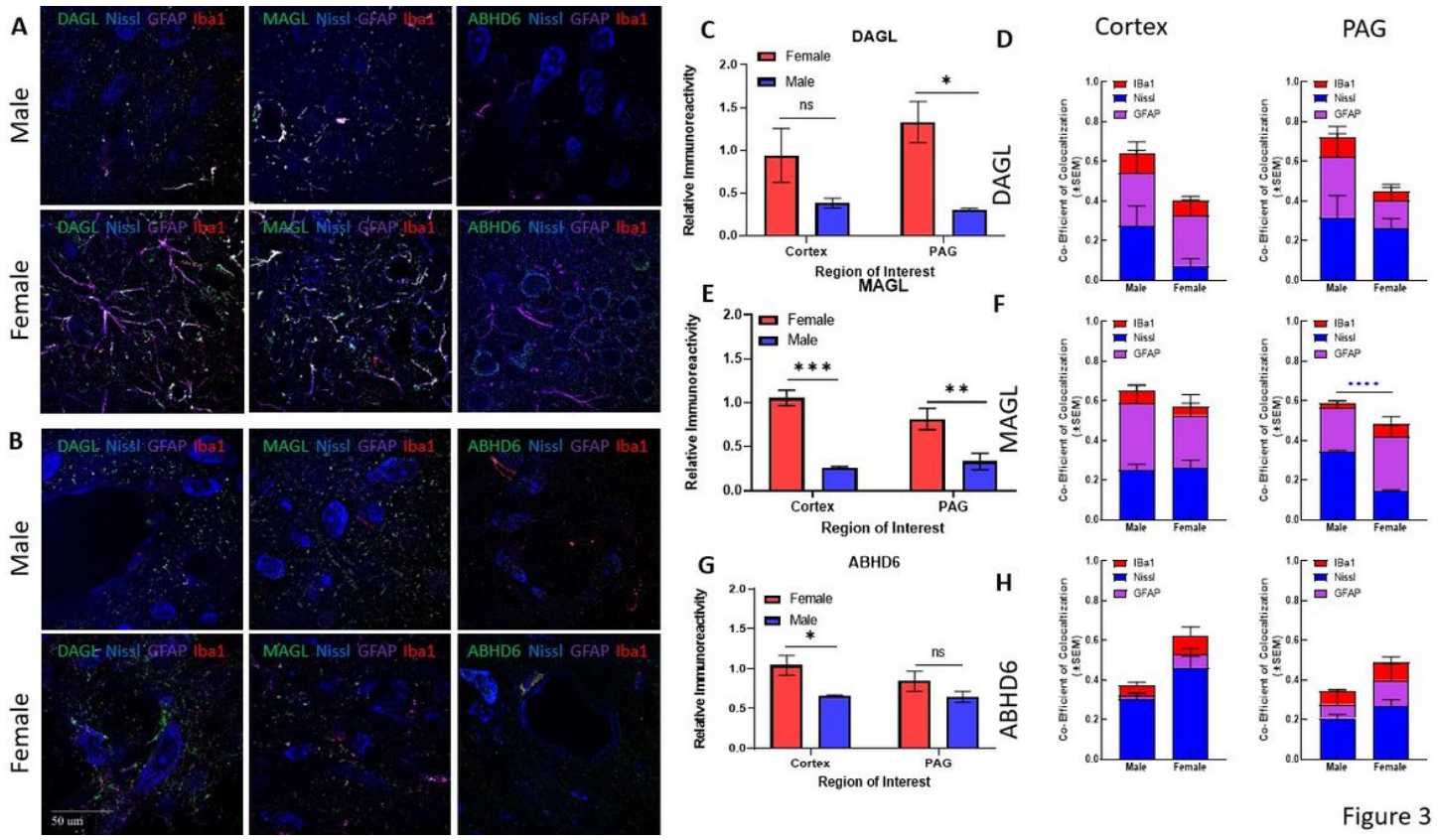

Figure 3

Figure 3

Immunohistochemical Analysis of the AEA System (A) Immunohistochemistry of naïve male and female V1M cortex. Staining for NAPE-PLD, FAAH, Iba1, GFAP, and Nissl was performed. Original magnification 63X. (B) Immunohistochemistry of naïve male and female PAG. Staining for NAPE-PLD, FAAH, Iba1, GFAP, and Nissl was performed. Original magnification 63X. (C) Measurement of relative area of IHC field occupied by NAPE-PLD staining pixels for each sex and region. Female NAPE-PLD immunoreactivity was significantly higher in PAG vs male PAG (*p=0.02) (D) Measurement of co-efficient of colocalization for NAPE-PLD with IBa1, Nissl, and GFAP. NAPE-PLD colocalized with Nissl at significantly higher rates in Female V1M cortex vs male V1M cortex (****p=0.001). No significant differences observed in PAG. (E) Measurement of relative area of IHC field occupied by FAAH staining pixels for each sex and region. FAAH immunoreactivity was significantly higher in female PAG vs male PAG (***p=0.0042) as well as female PAG vs female V1M cortex (###p=0.002) (F) Measurement of co-efficient of colocalization for FAAH with IBa1, Nissl, and GFAP. No significant differences observed between region or sex. All calculations for co-efficient of colocalization were performed with respect to the relevant enzyme. N=3/sex for each analysis.

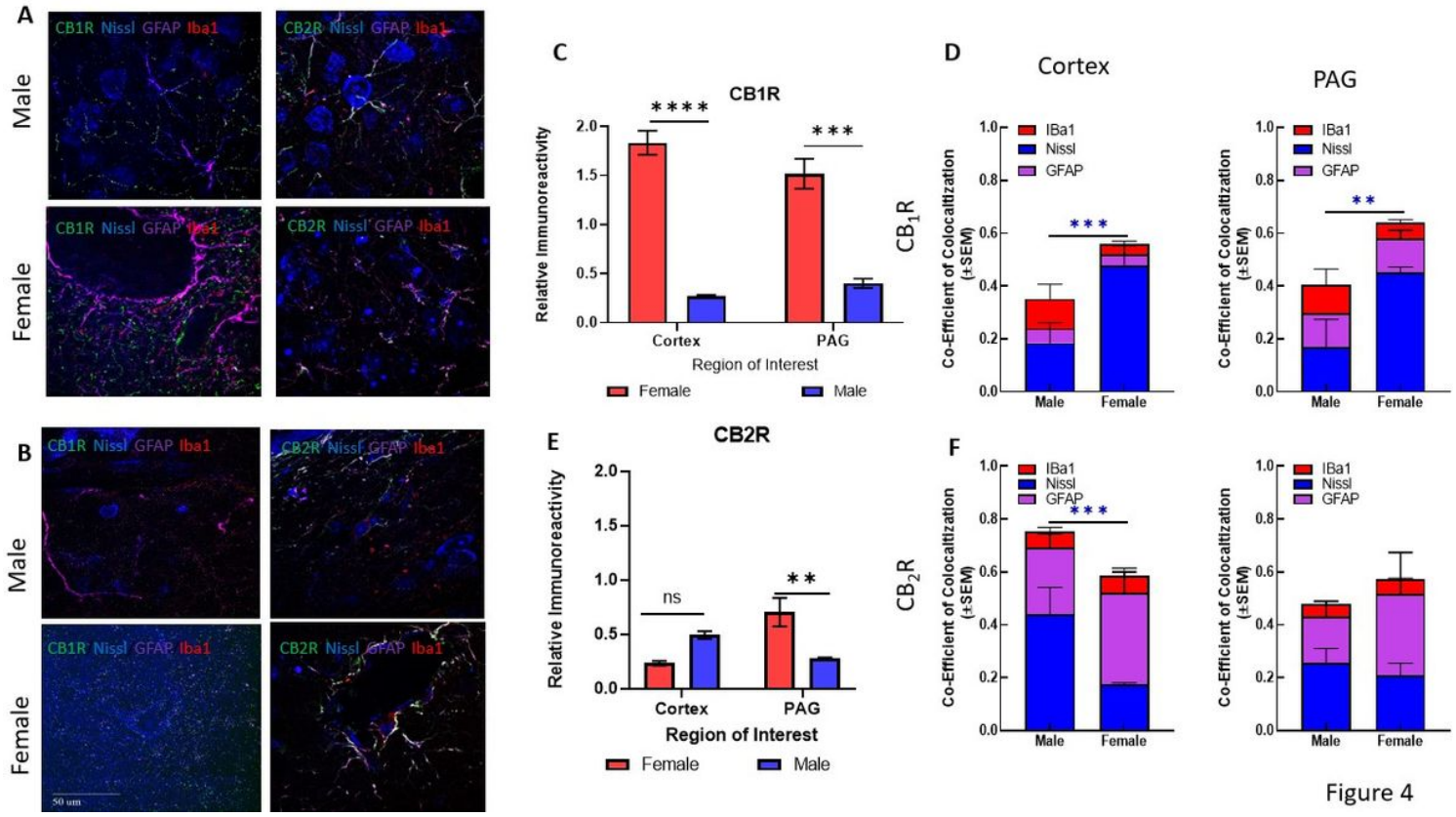

Figure 4

Figure 4

Immunohistochemical Analysis of CB1R and CB2R (A) Immunohistochemistry of naïve male and female cortex. Staining for CB1R, CB2R, Iba1, GFAP, and Nissl was performed. Original magnification 63X. (B) Immunohistochemistry of naïve male and female PAG. Staining for CB1R, CB2R, Iba1, GFAP, and Nissl was performed. Original magnification 63X. Scale on lower left image applies to all frames (C) Relative immunoreactivity of CB1R staining revealed significantly greater staining for CB1R in female cortex and lPAG vs males for both regions (****p<0.0001 female cortex vs male cortex, ***p=0.001 female lPAG vs male lPAG) (D) Measurement of co-efficient of colocalization for CB1R with Iba1, Nissl, and GFAP. CB1R colocalization with Nissl was significantly higher in female Cortex vs male Cortex (***p=0.008) and female PAG vs male PAG (**p=0.01) (E) CB2R immunoreactivity was significantly higher in female lPAG vs male lPAG (**p=0.0053) (F) Measurement of co-efficient of colocalization for CB2R with IBa1, Nissl, and GFAP. CB2R colocalization with Nissl in the male cortex was significantly greater than in female cortex (***p=0.0178). All calculations for co-efficient of colocalization were performed with respect to the relevant enzyme. N=3/sex for each analysis.

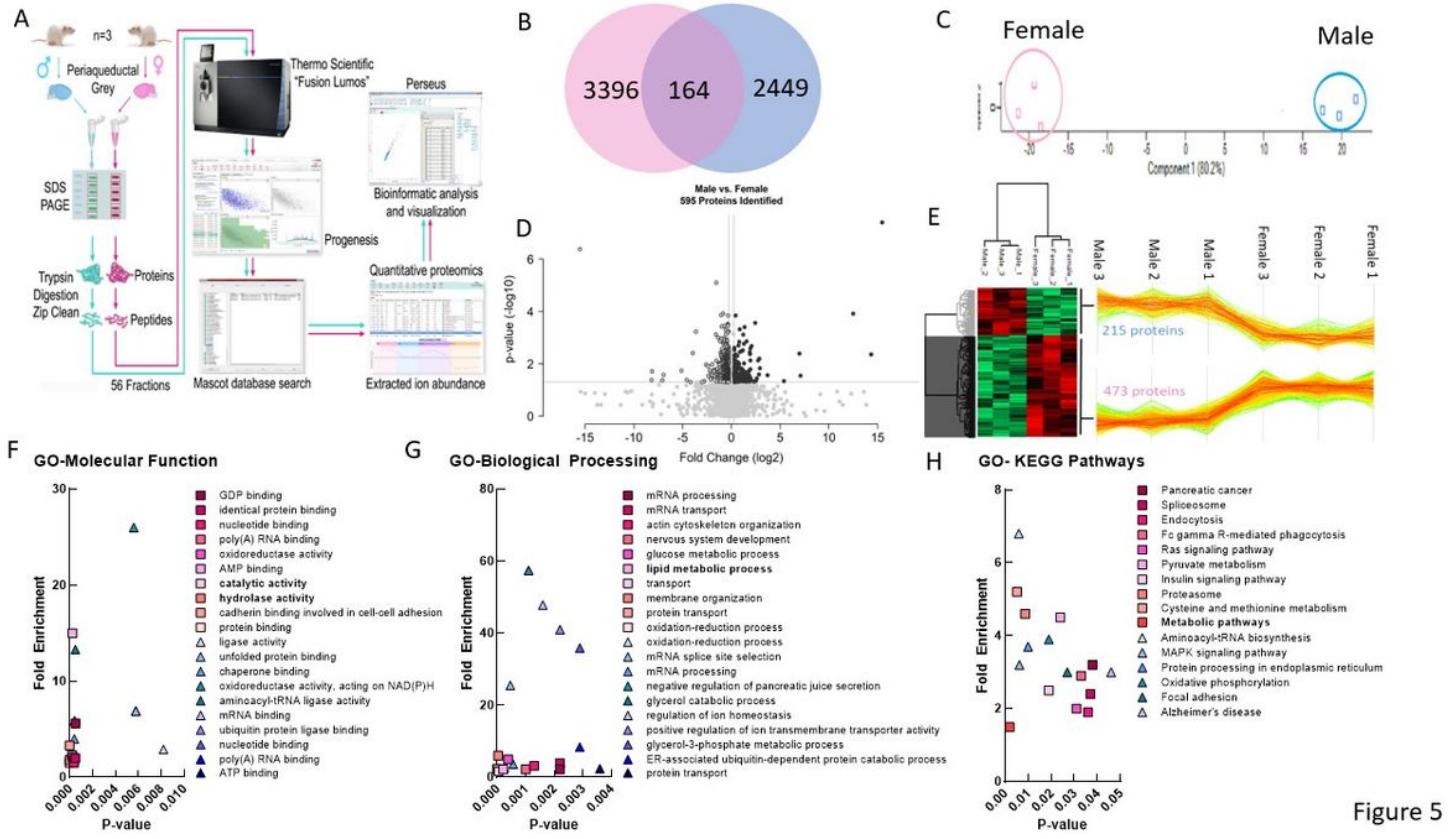

Figure 5

Proteomic analysis of naïve male and female PAG samples (A) Schema of proteomic analysis (B) Venn Diagram of male vs. female sex differences in proteins detected (C) (D) (E) Gene ontology (GO) enrichment analysis of the significantly affected proteins (F) GO-Molecular Function analysis (G) GO-Biological Processing analysis (H) GO-KEGG Pathway analysis

Supplementary Files

This is a list of supplementary files associated with this preprint. Click to download.

- AdditionalFigure1.jpg
- eCBsexdiffAddlTables110.xlsx